Identification of a trafficking motif involved in the stabilization and polarization of P2X receptors.

Séverine Chaumont-Dubel, Lin-Hua Jiang, Aubin Penna, R Alan North, A. Baranski

Identification of a Trafficking Motif Involved in the Stabilization and Polarization of P2X Receptors

Séverine Chaumont[1], Lin-Hua Jiang[2], Aubin Penna[1], R. Alan North[2] and Francois Rassendren[1*]

Running title: trafficking motif of P2X ATP-gated channels

[1]Département de Pharmacologie, Laboratoire de Génomique Fonctionnelle, CNRS UPR2580. 141, rue de la Cardonille, 34396 Montpellier France

tel +33 499 61 99 78

fax +33 499 61 99 01

[2]Institute of Molecular Physiology, University of Sheffield, Western Bank, Sheffield S10 2TN, U.K.

* corresponding author, far@igh.cnrs.fr

Abstract

Extracellular ATP-gated channels (P2X receptors) define a third major family of ionotropic receptors, and they are expressed widely in nerve cells, muscles, endocrine and exocrine glands. P2X subunits have two membrane-spanning domains and a receptor is thought to be formed by oligomerization of three subunits. We have identified a conserved motif in the cytoplasmic carboxy termini of P2X subunits that is necessary for their surface expression: mutations in this motif result in a marked reduction of the receptors at the plasma membrane because of a rapid internalization. Transfer of the motif to a reporter protein (CD4) enhances the surface expression of the chimera, indicating that this motif is likely involved in the stabilization of P2X receptor at the cell surface. In neurons, mutated $P2X_2$ subunits showed reduced membrane expression and an altered axodendritic distribution. This motif is also present in intracellular regions of other membrane proteins, such as in the third intracellular loop of some G protein-coupled receptors, suggesting that it might be involve in their cellular stabilization and polarization.

Keywords: ion channels / P2X receptors / stabilization / surface expression / polarization

P2X receptors are extracellular ATP-gated ion channels; they define a third major class of ligand-gated channels together with the glutamate and the nicotinic super-families (1). P2X receptors are involved in synaptic transmission in central and peripheral nervous system; but, in contrast to other ligand-gated channels, they are also widely expressed in peripheral tissues where they participate in physiological processes as diverse as smooth muscle contraction, secretion, and bone resorption. ATP induced currents have been recorded from a large number of different cell types (2) but the molecular identity of P2X receptors responsible for these currents often remains elusive because of limitations of pharmacological tools to discriminate the different subtypes of P2X channels.

Seven P2X subunits genes ($P2X_1$-$P2X_7$) are found in the human genome; this number seems to be an accurate estimation of the extent of the P2X family in mammalian species, although in zebrafish two additional subunits appear to exist (2,3). The basic structural determinants of P2X channels been established by numerous molecular studies (4). P2X subunits have a membrane topology with two transmembrane domains linked by a large extracellular loop, N- and C-termini are localized intracellularly (5,6). To form a channel P2X subunits are thought to associate as a homo- or hetero-oligomers, composed of three subunits (7,8) organized in a head-to-tail orientation around a central pore (9). This model is consistent with studies which show that the permeation pathways is associated with transmembrane regions (10-12), and with the fact that the gating of the channel is in part due to movements of the subunits relative to the each other (12). Conserved charged residues in the extracellular loop have been implicated in ATP binding (13,14), and desensitization is tightly linked to transmembrane domains and intracellular regions localized immediately beneath the plasma membrane (15,16).

Signals that regulate intracellular trafficking of P2X receptors are not well understood. In $P2X_4$ subunits, an atypical endocytosis motif responsible for the rapid recycling of the receptor has been identified in the carboxy terminus of the channel (17,18); however, the existence of subcellular trafficking in other P2X subunits signals has not been reported. Yet evidence suggests that additional trafficking signals are present in P2X subunits. For example, transiently expressed $P2X_6$ subunits are not properly addressed to the cell surface presumably because of a glycosylation defect (19), and the presence of a retention signal in the rat $P2X_5$ subunit has been suggested to explain its poor functional expression (20). Different mutations that alter surface expression of P2X subunits have also been reported. Disrupting some of the conserved disulfide bridge of the extracellular loop of $P2X_1$ subunits alters their normal trafficking to the cell surface (21); similarly, the deletion of the three glycosylated asparagines of the $P2X_2$ subunits induces an intracellular retention and a complete loss of function of the receptors (5,22). However, these mutations are likely to alter the folding of the protein, and the trafficking defects might rather be due a failure to pass the quality check test that normally take place in the endoplasmic reticulum than to a trafficking defect *per se*. In the human $P2X_7$ receptor a dibasic amino acid motif (23) and a polymorphism (Ile^{568} to Asn) (24) both located in the C-terminal tail of the protein have been shown to be necessary for the proper trafficking of the channel. No mechanistic explanations have been put forward to explain these trafficking defects.

In the present study we have identified a motif in the C-terminal tail (C-Term)[1] of P2X subunits that is conserved in almost all subunits known to date. Using a chemiluminescence assay (25,26) to measure the cell surface expression of P2X subunits we show that in HEK cells and in neurons this motif is involved in the

stabilization at the plasma membrane of all P2X subunits tested ($P2X_2$, $P2X_3$, $P2X_4$, $P2X_5$ and $P2X_6$). We also provide evidence that this motif might be important for the polarized expression of $P2X_2$ receptors in neurons.

EXPERIMENTAL PROCEDURES

Insertions of extracellular tags on P2X receptors -- Tags were introduced by overlapping PCR as described previously (8) in the extracellular loop of P2X subunits, all at similar positions: Flag tags were inserted in $P2X_2$ and $P2X_6$ between D78-K79 and E83-K84, respectively; $P2X_3$ bears a Myc tag inserted between residues N104-R105, $P2X_4$ has a HA tag between Q78-L79 and $P2X_5$ has either a Myc or a HA tag inserted between T78-T79. In all cases tag Insertions did not alter the function of the different P2X subunits measured electrophysiologically. All constructs were confirmed by DNA sequencing.

Mutagenesis -- Mutations were introduced as described in (10) using the Quickchange (Stratagene) protocol. A mutagenized fragment was excised by restriction digestion and subcloned into the respective backbone P2X subunit. All mutants were confirmed by sequencing.

Construction of CD4 chimeras -- Human CD4 genes (hCD4-AAXX, hCD4-KKXX, hCD4-GFP-KKXX) were a kind gift of B. Schwappach (Zentrum fur Molekulare Biologie, University of Heidelberg). The C-terminus of $P2X_2$, $P2X_{2b}$ and $P2X_3$ were amplified with a forward primer containing an in frame *NotI* site. *NotI-XbaI* fragments were generated and sub-cloned in the different CD4 plasmids (CD4-AAXX, -KKXX, CD4-GFP-KKXX). All the clones were subsequently verified by sequencing.

Chemiluminescent assay -- Cells were transfected in 35mm dishes. Twenty four hours after transfection, each plate was divided into 4 wells of a 12-well plate.

Assays were carried out 48 h after transfection. Cells were fixed in 4% paraformaldehyde for 5 min and the cells in two of four wells in each case were permeabilized using 0.1% triton-X100. Cells were incubated in blocking solution PBS/1% fetal calf serum for 30 min and incubated with primary antibody for 1 h at room temperature. After extensive washing, cells were incubated for 20 min at room temperature with a secondary antibody coupled to peroxidase (1/1000: anti-mouse peroxidase conjugated, Amersham Biosciences). Luminescence was measured using Supersignal ELISA femto Maximum sensitivity substrate (Pierce) and quantified in a Victor 2 luminometer (Perkin Elmer).

For Flag- and HA-tagged constructs, we used a primary antibody directly coupled with peroxidase (1/4000: anti-Flag M2-peroxidase (Sigma) and 1/2000: anti-HA-peroxidase, clone 12CA5 (Roche)), thus eliminating the need for a secondary antibody. For other constructs, we used Myc antibody (1/1000: monoclonal anti-Myc antibody clone 9E10, Developmental Studies Hybridoma Bank) or CD4 antibody (1/100: monoclonal anti-hCD4, Immunotech). Surface expression was calculated as the ratio between the signal obtained for non-permeabilized cells (representing the amount of proteins at the cell surface), and the signal obtained for permeabilized cells (which represents the total cellular amount of proteins).

Cell culture and transfections -- HEK293 cells and COS cells were cultured in DMEM-Hepes containing 10% fetal calf serum, 1% glutamax and 1% penicillin plus streptomycin. Transfections were carried out in 35 mm dishes with a maximum of 1 μg of plasmid DNA, using lipofectamine2000 (Invitrogen) for HEK293 cells and JetPei (Qbiogen) for COS cells, according to the manufacturers' protocols. Hippocampal cultures were prepared from E17-E18 mice and grown in B27-supplemented Neurobasal (Gibco) medium on poly-L-ornithine and laminin pre-coated coverslips as

previously described. Ten day old cultures were transfected with P2X-GFP fusion protein using lipofectamine 2000 (Invitrogen): 1.5 µg DNA and 1.5 µl lipofectamine 2000 were each mixed with 50 µl neurobasal medium for 15 min and then mixed together and incubated for 30 min at room temperature. After addition of 150 µl neurobasal B27 the mixture was applied to the neuronal culture for 2 h at 37°C, 5% CO_2 and then replaced by fresh neurobasal B27. Neurons were studied 48h later. Data were collected from at least three different dishes prepared from at least three different cultures and transfections.

Immunofluorescence on HEK293 cells -- Immunofluorescence experiments were carried out 48 h after transfection. Cells were fixed in 4% paraformaldehyde for 5 min, blocked in PBS-0.5% BSA for 30 min and incubated for 1 - 2 h at room temperature with the primary antibody (1/1000: anti-Flag M2 biotinylated, Sigma) in blocking solution, and then for 20 min at 37°C with streptavidin Texas-Red (1/2000: APBiotech). For labeling living cells, cells were incubated in complete culture medium for 1 h with the primary antibody at 37°C following by incubation for 20 min at 37°C with streptavidin Texas-Red prior to fixation.

Immunofluorescence on COS cells and hippocampal neurons – Forty-eight hours after transfection, COS cells were fixed for 10 min at 37°C in 4% paraformaldehyde/4% sucrose. Cells were then washed in PBS 0.3%, BSA glycine 50 mM, and permeabilized at 37°C in blocking solution (PBS 0.05%, saponin 0.3%, BSA). Cells were incubated in blocking solution containing primary antibody at room temperature for 2 h and after extensive wash, cells were incubated for 20 min at 37°C with secondary antibody. For cells transfected with $P2X_2$-GFP fusion, anti-calreticulin (1/200: Alexis Biochemicals) and Cy3-conjugated anti-rabbit secondary antibody (1/1000: Jackson ImmunoResearch) were used. For cells transfected with

CD4-GFP-KKXX and Flag-$P2X_2$ receptors, we used biotinylated anti-Flag M2 antibody (1/1000: Sigma) and streptavidin-Texas Red (1/2000: APBiotech). Fluorescence was visualized on a Leica DMRA2 epifluorescent microscope using an x40 oil immersion objective. Images were acquired using a cool-snap HQ (photometrics) digital camera.

Internalization experiments -- HEK293 cells stably expressing $P2X_2$, $P2X_2$[K366A] or $P2X_2$[Y362A] were grown on polyornithine coated cover slips for 24 h. To monitor receptor internalization cells were incubated at 37 °C for 30 min in DMEM-Hepes containing monoclonal anti-Flag M2 antibody (1/1000: Sigma) and 100μg/ml leupeptin. The cells were then placed on ice and fixed in 4% paraformaldehyde for 5 min. Cover slips were transferred in a PBS solution containing 0.3% BSA and 192 mM glycine for 15 min at room temperature to quench paraformaldehyde fluorescence. After an additional 30 min blocking in PBS/0,3% BSA, surface staining was achieved for 20 minutes at 37 °C with an FITC-conjugated anti-mouse secondary antibody (1/1000: Chemicon) in PBS 0.3% BSA blocking solution. Cells were then permeabilized for 5 min in 0.01% Triton X-100 and internalized receptors/antibodies complexes were measured following a 20 min incubation at 37 °C in the presence of a Cy3-conjugated anti-mouse secondary antibody (1/2000: Jackson laboratories) in PBS 0.3% BSA. Fluorescence was visualized using a Leica TCS SP2 confocal inverted microscope with a Nikon 63x1.32 HCX planapochromatic objective. FITC was excited with an argon laser at 488 nm, Cy3 was excited with a helium/neon at 543 nm. Images were collected sequentially to avoid cross contamination between fluorochromes. Series of optical sections were scanned at a 1024x1024 pixels resolution and collected in the Leica confocal software. 8-bit TIFF images were imported and analyzed with ImageJ 1.62 (NIH).

Electrophysiological recordings -- HEK293 cells were used to express the wild type and mutant P2X receptors with green fluorescent protein as described above. A plasmid ratio of 1:5 was adopted for co-expression of $P2X_2$ and $P2X_3$ subunits. Whole cell recordings were carried out at room temperature using an EPC9 patch clamp amplifier (HEKA Elektronik, Germany) as detailed previously and briefly described below. Membrane potential of the patched cells was held at –60 mV. Extracellular solution contained (in mM): 147 NaCl, 2 KCl, 1 $MgCl_2$, 2 $CaCl_2$, 10 HEPES and 13 glucose. Intracellular solution contained (in mM): 147 NaF, 10 HEPES, and 10 EGTA. These solutions were maintained at pH 7.3 and 300 - 315 $mosmol^{-1}$. Agonists were applied using an RSC 200 fast-flow delivery system (Biologic Science Instruments, France). The current responses from individual cells were normalized to cell membrane capacitance (in a range of 8 - 20 pF) and presented as current density (in pA/pF). All data are presented where appropriate as mean ± s.e.m..

RESULTS

Identification of an intracellular motif implicated in the surface expression of the $P2X_2$ receptor -- The carboxy terminal region of rat P2X subunits have different lengths, ranging from 27 amino acids for $P2X_6$ to 240 for $P2X_7$. As show in Fig. 1A, their alignment in the immediate juxtamembrane region shows little homology, but two amino acids are completely conserved. This motif YXXXK is located eight residues downstream of the end of the second transmembrane domain in all except the $P2X_7$ subunit, where an extra 18 amino acids cysteine rich domain is intercalated. In most subunits the residue preceding the conserved lysine is also a basic residue;

we therefore investigated if this motif YXXXK could be implicated in P2X receptor trafficking. To that aim we used P2X subunits in which epitope tags were introduced in the extracellular loop in a position that did not modify noticeably receptors properties (8).

Mutation analysis of $P2X_2$[Y362A] and $P2X_2$[K366A] -- HEK cells were transfected with either $P2X_2$, $P2X_2$[Y362A] or $P2X_2$[K366A] cDNAs carrying an extracellular Flag tag; expression of the channels was analyzed two days later by immunofluorescence either in living cells or after fixation and permeabilization. As shown in Fig. 1B, mutation to alanine of either Y362 or K366 strongly decreases immunostaining of the receptors as compared to wild type (Wt) subunits suggesting that the surface expression of mutated subunits is affected; when cells were permeabilized, immunofluorescence of mutated subunits was apparently not different from Wt $P2X_2$ (not shown). Because immunofluorescence is not quantitative and does not allow for detection of subtle changes in protein expression, we have used a luminescent-based assay that gives a direct and accurate quantification of the expression of proteins. Depending upon the permeabilization state of the cells, this approach allows the quantification of cell surface expressed receptors (non-permeabilized state, NP) or of the total cellular content of the protein (permeabilized state, P). In addition, the quantification of the total cellular amount of the protein provides a direct indication of the stability of mutated subunits.

As shown in Fig. 1C, in non-permeabilized conditions the luminescent signal was strongly reduced for cells expressing $P2X_2$[Y362A] or $P2X_2$[K366A] subunits as compared to cell transfected with Wt $P2X_2$. No difference in the total amount of mutant protein was observed. The ratio NP/P indicates that 73 ± 16% (n = 9) of Wt $P2X_2$ receptor were present at the plasma membrane but only 34 ± 5.5 % (n = 7) and

28 ± 4.5% (*n* = 7) for $P2X_2$[Y362A] and $P2X_2$[K366A], respectively. The double mutant $P2X_2$[Y362A,K366A] did not show any further decrease in the receptor surface expression (data not shown).

We next studied whether other residues in the vicinity of the YXXXK motif could also interfere with the surface expression of the $P2X_2$ subunit. Residues downstream of the second transmembrane region, from K360 to K369, were individually mutated to alanine and their membrane expression examined. As shown in Fig. 1D, none of these mutants showed any decreased membrane expression; nor did the mutation to alanine of the two leucines (L354, L355) located at the end of the second transmembrane domain (data not shown). These results indicate that the YXXXK motif plays an important role in the trafficking of the $P2X_2$ subunit to the plasma membrane.

Specificity of the YXXXK motif and functional characterization of mutant subunits -- Additional amino acids substitutions were introduced at the Y362 and K366 positions (Y to F; K to R, K to G and K to Q). All mutants were individually transfected in HEK cells and membrane expression quantified by chemiluminescent assay. Fig. 2A shows that all mutants had reduced surface expression ranging from 22 ± 6.2% (*n* = 3) for K366Q to 43 ± 3.5% (*n* = 3) for Y362F; even when the conservative substitutions Y362F and K366R were introduced surface expression of the receptor was still decreased. These values were not different from what was observed for membrane expression of Y362A and K366A.

We next investigated if the introduced mutation at both Y and K positions had any consequences on ATP-evoked currents in HEK transfected cells. Because a 20 to 40% residual membrane expression of these mutants was consistently observed, we expected to observe similar reduction of the ATP current densities. As shown in

Fig. 2B, the mutations introduced at Y362 and K366 positions had different phenotypes. When either alanine or phenylalanine were introduced at the Y362 position ATP was still able to induce currents. Currents densities were reduced from 175 ± 29 (n = 9) pA/pF for Wt $P2X_2$ to 62 ± 12 (n = 6) pA/pF and 58 ± 23 (n = 5) pA/pF for $P2X_2$[Y362A] and $P2X_2$[Y362F] respectively (Fig. 2C). These values are similar to what we observed in terms of reduction of the surface expression of these mutants. In the case of the Y362A mutation, a second application of ATP (30 μM) did not induce any current, indicating a strong desensitization of the current (data not show). This not observed with the more conservative substitution Y362F. Cells transfected with substitutions at the K366 positions did not produce any current in response to ATP (concentrations up to 1 mM), although they had residual surface expression of around 30% (Fig. 2B). These results are in agreement with a previous report in which $P2X_2$[K366Q] was shown to be non-functional (27).

The lack of function of $P2X_2$ K366 mutants might be due to a disruption of the oligomeric organization of the channel and subsequently its trafficking to the cell surface. To test this hypothesis we performed co-immunoprecipitation between Wt $P2X_2$ and $P2X_2$[K366A] subunits. Receptor complexes were immunoprecipitated through the Flag epitope present one subunit and the presence of the second subunit was detected owing to its Myc epitope. In all situations, including the homomeric $P2X_2$[K366A] complex, co-immunoprecipitation of subunits was successfully obtained (Fig. 2D). These results demonstrate that the decreased surface expression of $P2X_2$[K366A] subunit and its lack of function cannot be attributed to an inability of the mutant to oligomerize with itself or with other subunits.

The YXXXK motif regulates surface expression of other P2X subunits -- The YXXXK motif is conserved in almost all P2X subunits cloned to date; we therefore

asked whether the mutation of this motif in other P2X subunits would also impair their surface expression. Mutations to alanine of the Y and K residues were individually introduced in Myc-$P2X_3$, HA-$P2X_4$, HA-$P2X_5$ and Flag-$P2X_6$ subunits. Membrane expression of these different mutants and of their respective wild type subunits was measured by chemiluminescence assay (Fig. 3A). Mutation of either tyrosine or lysine residues in all P2X subunits caused a large decrease of surface expression when compared to the respective wild type subunits; surface expression levels of mutated subunits were all in the same range, excepting $P2X_6$: $P2X_3$[Y353A] 27 ± 5.3% (*n* = 3), $P2X_3$[K372A] 23 ± 0.3% (*n* = 3), $P2X_4$[Y367A] 36 ± 6.4% (*n* = 4), $P2X_4$[K370A] 27 ± 7.2% (*n* = 4), $P2X_5$[Y369A] 34 ± 6% (*n* = 5), $P2X_5$[K372A] 37 ± 4.3% (*n* = 5), and $P2X_6$[K365A] 58 ± 3.5% (*n* = 4). In all cases, the total cellular amount of protein was not altered (data not shown), indicating that a decrease of the stability mutant P2X subunits could not be accounted for the observed decrease in their surface expression.

Recordings from ATP-induced currents in HEK cells transfected with $P2X_3$, $P2X_4$ and $P2X_5$ tyrosine and lysine mutants showed that none of them responded to ATP, even at concentrations up to 1 mM. By comparison, when wild type subunits were used in the same experiments, normal currents were observed (see figure 3B). The ATP analog αβ-methylene-ATP (αβmeATP) was also ineffective to induce current in HEK cells transfected with $P2X_3$[Y353A] and $P2X_3$[K357A] mutants Of the eight P2X mutant subunits tested, only $P2X_2$[Y362F] and $P2X_2$[Y362A] showed any functional response to ATP: in the latter case the currents desensitized markedly.

Surface expression of mutant P2X subunit is rescued by wild type subunits -- $P2X_2$ and $P2X_3$ subunits form well characterized hetero-oligomeric receptors with pharmacological and biophysical properties that are clearly distinct from homo-

oligomeric $P2X_2$ and $P2X_3$ channels (28,29). We studied the trafficking of heteroligomeric P2X receptors formed by the association of wild type and trafficking deficient subunits. As show in Fig. 4A, when Flag-$P2X_2$[K366A] was co-expressed with non-tagged $P2X_3$ subunits, a strong surface immunostaining of the mutant $P2X_2$ was recovered. Quantification of the recovery by chemiluminescent assay confirmed that when $P2X_2$[K366A] was co-expressed with $P2X_3$ 80% ± 6.7 (*n* = 4) of the total cellular amount of the subunit was expressed at the cell surface, compared to only 32% ± 1.0 (*n* = 4) when $P2X_2$[K366A] was expressed alone. Similar results were found when $P2X_2$[Y362A] was co-expressed with $P2X_3$ (data not shown). In the converse experiment, when the Myc-tagged $P2X_3$[K357A] subunit was co-expressed with the non-tagged $P2X_2$ subunit its surface expression rose from 23% ± 0.3 (*n* = 3) ($P2X_3$[K357A]) to 79% ± 4.9 (*n* = 3) ($P2X_3$[K357A]/$P2X_2$) (Fig. 4C).

Electrophysiological recordings were performed to determine if the co-expression of $P2X_3$ with $P2X_2$[K366A] could rescue the lack of function of $P2X_2$ mutant subunit. Fig. 4B shows that when $P2X_2$[K366A] subunit was co-expressed with the $P2X_3$ subunit, $\alpha\beta$meATP induced currents that desensitize slowly compared to $P2X_3$ currents. The hetero-oligomeric current was isolated by measuring the amplitude of the currents evoked by $\alpha\beta$meATP (30 μM) 2 s after the start of the agonist application; this is expressed as a percentage of the peak current. For $P2X_2$[K366A]/$P2X_3$ receptors currents at 2 s were 37% ± 3.0 (*n* = 7) of the peak current, compared to 77% ± 3.1 (*n* = 13) and 3.3% ± 0.8 (*n* = 6) for $P2X_{2/3}$ and homo-oligomeric $P2X_3$ channels, respectively. These values indicate that Wt $P2X_3$ also rescues the function of $P2X_2$[K366A] mutant. However, the reciprocal was not true. When $P2X_2$ wild type subunit was co-expressed with the $P2X_3$K357A mutant, no currents could be induced with 30μM $\alpha\beta$meATP. This was somewhat surprising

since 78% of $P2X_3$[K357A] was expressed at the surface expression when co-expressed with the wild type $P2X_2$ (Fig. 4A). One likely explanation is that the $P2X_3$ subunit is dominant in $P2X_{2/3}$ receptors, and implies that in a hetero-oligomeric channel the dominant subunit needs to be itself functional to enable the oligomeric channel to operate (9) .

Mutation of the YXXXK motif does not induce retention of $P2X_2$ subunits in the endoplasmic reticulum -- Immunofluorescence and luminescence data clearly indicated that $P2X_2$[Y362A] and $P2X_2$[K366A] subunits as well as the other P2X mutant subunits were not expressed at the cell surface but are present intracellularly. One possibility is that the mutation of the YXXXK motifs impaired the transport of the receptor to the plasma membrane and induces its retention in an intracellular compartment. We therefore investigated if Wt and mutant $P2X_2$ subunits showed different intracellular localization. COS-7 cells were transiently transfected with $P2X_2$-GFP fusion constructs containing or not the [Y362A] or the [K366A] mutations. Cells were fixed 48 h after transfection and endoplasmic reticulum was labeled with an anti-calreticulin antibody for co-localization experiments. As shown in Fig. 5A, in COS-7 cells expressing $P2X_2$-GFP, the protein is localized at the plasma membrane as well as in intracellular compartments that are labeled by the anti-calreticulin antibody. In cells transfected with mutant $P2X_2$-GFP subunits no GFP signal could be resolved at the plasma membrane, whereas it clearly co-localizes with calreticulin. No difference is observed in the intracellular localization of Wt and mutant subunits. This was further observed when a CD4-GFP fusion protein that carried a C-terminal KKXX ER retention motif (25) was co-expressed with Flag-P2X2 Wt or mutant subunits (data not shown). In addition, co-labeling experiments with markers of the trans-Golgi network did not revealed any differences between Wt and mutant $P2X_2$

subcellular localization. Because in transient transfection the synthesis of the recombinant protein is constant, it is difficult to discriminate using classical immunofluorescent approaches between proteins that are retained in intracellular compartments such as the endoplasmic reticulum from proteins being normally shipped to their terminal location. To circumvent this problem we performed glycosylation analyses to monitor a possible ER-to-Golgi transport defect in mutant $P2X_2$ subunits. Fig. 5B illustrates pulse-chase assays which demonstrate that both Wt and mutant $P2X_2$ subunits were able to acquire endo-H resistant carbohydrates after a 1 or 3 h chase period. No differences in the endoH sensitivity could be observed between Wt and mutant subunits at these different time points, ruling out a difference in the rate of transport between compartments of mutant and Wt subunits. These results indicate that mutant P2X subunits are not retained in the ER and that their transport is not likely to be affected.

Increased internalization of P2X2 trafficking deficient subunits -- One possible explanation for the reduced surface expression of mutant P2X subunits might be that these subunits are not stabilized at the plasma membrane but rapidly cycle between the cell surface and the intracellular compartment. To test this hypothesis we monitored endocytosis of Wt and mutant Flag-tagged $P2X_2$ subunits expressed in stable HEK cells. Internalization of $P2X_2$ subunits was measured after incubation of cells for 30 min at 37 °C with an anti-Flag antibody. Non-internalized receptors were detected using a FITC-labeled secondary antibody with prior permeabilization, whereas the internalized pool of anti-Flag bound-receptors were labeled with a Texas Red-labeled secondary antibody after permeabilization. This approach has been used to monitor $P2X_4$ constitutive internalization in HEK cells as well as in neurons (17). As a positive control for receptor internalization, HEK cells transiently

transfected with HA-tagged $P2X_4$ receptor cDNA were used. As shown in Fig. 6A, Wt $P2X_2$ receptors show very little internalization; strong extracellular labeling of tagged-receptor was obtained after 30 min incubation with the anti-Flag antibody whereas almost no internalized-labeled receptor could be detected. By contrast, under identical conditions HEK cell expressing either $P2X_2$[Y362A] or $P2X_2$[K366A] subunits display reduced extracellular staining and a punctated intracellular receptor labeling. Similar intracellular staining was observed for $P2X_4$ expressing cells (not shown). In control experiments in which cells were fixed but not permeabilized, addition of the Texas Red-labeled secondary antibody gave almost no signal indicating that all extracellular epitopes were saturated (not shown). These results demonstrate that $P2X_2$[Y362A] or $P2X_2$[K366A] receptors reach the plasma membrane but rapidly internalized presumably through fluid phase membrane internalization. One can reasonably propose that mutant P2X receptors are not stabilized at the plasma membrane and that the YXXXK motif is necessary for their membrane stabilization through interactions with cytoskeletal proteins.

The YXXXK motif enhances surface expression of CD4 -- We next asked if the YXXXK motif of P2X receptor could stabilized the surface expression of unrelated membrane proteins. To that aim we fused wild type or mutated C-termini tails to CD_4 intracellular extremity (see Fig. 6B); surface expression of Wt CD_4 and CD_4-P2X chimera were measured by chemiluminescence assay after transfection in HEK cells. When the $P2X_2$ C-Term was fused to CD_4 its surface expression increased by 38% ± 7.3 (*n* = 6) as compared to Wt CD4 (Fig. 6B). However this increase was not observed in subunits where the YXXXK motif of the $P2X_2$ C-Term was disrupted by mutation of either the tyrosine or the lysine residues. In this case we even observed a reduction of the surface expression of the CD_4-$P2X_2$ fusion protein (76% ± 16.8, *n* =

4) and 72% ± 7.3 (*n* = 4) for the tyrosine and the lysine mutants, respectively). $P2X_2$ C-terminus is 129 amino acids long and contains a 69 amino acids long alternative proline-rich exon that could be responsible for the reduction membrane expression of the mutated CD4-$P2X_2$ protein (30). We tested this hypothesis by using the C-terminal tail of the $P2X_{2b}$ subunit which lacks this exon (30). Surface expression of the CD_4-$P2X_{2b}$ was increased to 138 % ± 4.3 (*n* = 4) when compared to CD4; the disruption of the YXXXK motif abolished this increase, and surface expression of CD4-$P2X_{2b}$ was not different from Wt CD4 (105 % ± 12.4 (*n* = 3) and 102% ± 11.6 (*n* = 3) for the tyrosine and the lysine mutants, respectively). In a third experiment, the 43 amino acid long $P2X_3$ C-terminal tail was fused to CD4. We observed essentially the same result: CD_4-$P2X_3$ surface expression was 126% ± 7.0 (*n* = 5) compared to CD_4, whereas disruption of either of the two key residues of the YXXXK motif abolished this increased (surface expression was 99% ± 4.4 (*n* = 5) and 97% ± 5.2 (*n* = 5) for the tyrosine and the lysine mutants, respectively)(Fig. 5A). All together, these results clearly indicate that the YXXXK motif of P2X subunits enhances the surface expression of the unrelated CD4 membrane protein most likely by enhancing its stabilization at the plasma membrane.

Trafficking deficient P2X2 subunits have altered surface expression and axo-dendritic localization in neurons -- P2X receptors are expressed in different types of neurons in the central and peripheral nervous systems. We have therefore determined whether the surface expression of mutant $P2X_2$ subunits were similarly affected in neurons. Cultures (9 to 10 days) of embryonic hippocampal neurons were transfected with Wt or mutant Flag $P2X_2$-GFP cDNAs and studied 48 h later. Surface expression of receptors was studied using an anti-Flag antibody on non-permeabilized neurons whereas total receptor expression was visualized using GFP

fluorescence. As shown in Fig. 7A, neurons transfected with Wt $P2X_2$-GFP Flag staining (corresponding to cell surface expressed receptors) and GFP fluorescence (corresponding to all receptors) were found to be nearly identical in appearance. Fluorescence was observed in varicosities even in the distal regions of neuronal processes. However, when neurons were transfected with either $P2X_2$[Y362A]-GFP or $P2X_2$[K366A]-GFP subunits, a strong reduction of extracellular Flag staining was observed in the varicositises; the GFP signal remained not different from control. The number of varicosities that were double positive for Flag and GFP signals were quantified in neurons transfected with Wt and mutants $P2X_2$ receptors. Only 14% ± 2.9 (*n* = 13) and 11% ± 2.4 (*n* = 24) of varicosities were double positive for P2X2[Y362A] or P2X2[K366A] mutants respectively, whereas the corresponding figure for Wt $P2X_2$ was 43% ± 4.2 (*n* = 25). This clearly indicates that in neurons mutant $P2X_2$ subunits have a reduced membrane expression although their transport to varicosities seems not affected.

Because in neurons trafficking of ion channels is often linked to their polarized expression, we have determined if Wt and mutant $P2X_2$ subunits had a similar axo-dendritic localization in neurons. Dendritic expressed $P2X_2$ were visualized by co-localization experiments with the dendritic marker MAP2. As shown in Fig. 7B, after transfection Wt $P2X_2$-GFP receptors are expressed almost exclusively in dendrites. Indeed, in co-localization experiments GFP fluorescence is found only in MAP2 positive processes. However, when $P2X_2$[Y362A]-GFP or $P2X_2$[K366A]-GFP were transfected into neurons, GFP signal was observed in processes that were not MAP2 positive (see Fig. 7B) as well as co-localized with MAP2 positives dendrites. These results indicate that in neurons the YXXXK motif is not only necessary for surface expression of $P2X_2$ receptors but also for their polarized expression.

DISCUSSION

A conserved intracellular motif regulates the surface expression and the function of P2X subunits -- Sequences of the cytoplasmic carboxy terminal regions of P2X subunits are quite variable in length and minimally related to each other. However, alignment of the subunits in the region close to the end of the second transmembrane domain, shows that a tyrosine and a lysine separated by three amino acids are conserved. This defines a YXXXK motif present in 39 out of the 41 full length P2X sequences found in databases. This motif is not found only in two zebrafish subunits ($P2X_2$ and $P2X_{514}$)(3), but it is found in the three Dictyostelium P2X related sequences.

Our present results demonstrate that the YXXXK motif is responsible for appropriate surface expression of $P2X_2$, $P2X_3$, $P2X_4$, $P2X_5$ and $P2X_6$ receptors. Mutation to alanine of either conserved residues also leads to a loss of function of most the mutant channels. Although we cannot exclude that the loss of function and the reduced surface expression of mutant P2X subunits are directly related, several lines of evidence suggest that this is not the case. Indeed, three mutants $P2X_2$[Y362A] and $P2X_2$[Y362F] as well as $P2X_1$[Y363F] (31) retained residual activity (see Fig. 2) even though their surface expression was reduced. In addition, hetero-oligomeric channels formed by the association of Wt $P2X_2$ and mutant $P2X_3$ subunits are still not functional although both subunits have a normal surface expression (see below). This excludes a direct causality between the lack of functional expression of mutated subunits and their trafficking deficit. We cannot interpret the lack of function of the mutant subunits. One possibility is that these residues are involved in the regulation of the desensitization of the channels. Indeed, in the case of $P2X_2$[Y262A] mutant we observed that a single application of 30 μM ATP completely desensitizes

the channel. Similar findings were previously made on $P2X_1$[Y363F] mutant (31). In addition, several studies have demonstrate that the rate of desensitization of $P2X_2$ currents is modulated when mutations are introduced in the region downstream of the second transmembrane domain (15,27). It is possible that mutations introduced in the YXXXK motif in P2X subunits induce conformational changes to the receptor that correspond to a desensitized state. Alternatively, the YXXXK motif might be necessary for interactions with cytoskeletal proteins that normally regulate the desensitization of these channels. Such interactions have been shown to regulate the desensitization of $P2X_1$ receptors (32).

Trafficking rescue of mutant P2X subunits -- P2X receptors are oligomers probably composed of three subunits (7) that assemble either homo-oligomers or hetero-oligomers. $P2X_{2/3}$ hetero-oligomeric channels has been extensively studied (28,29). Based on biochemical and functional evidence it has been recently proposed that $P2X_{2/3}$ receptor is formed by the head-to-tail association of one $P2X_2$ and two $P2X_3$ subunits (9). Our results show that the surface expression of $P2X_3$[K357A] can be efficiently rescued by co-expression with the Wt $P2X_2$ or $P2X_3$ subunits. Taking the proposed $P2X_{2/3}$ subunits arrangement as valid, this suggests that one $P2X_2$ subunit is sufficient to stabilize the whole channel complex at the cell surface. Similar rescue of the surface expression of trafficking deficient ion channel by Wt subunits have been reported for the homo-oligomeric Kir2.1 and hetero-oligomeric Kir3 inward rectifier potassium channel (33). Kir channels have a tetrameric subunit organization; however, the number of Wt Kir subunits that are sufficient to drive the surface expression of the channel complex has not been documented. Our results suggest that one could be sufficient if the trafficking of P2X receptors and Kir channels follow the same general rules.

Functional rescue of trafficking-deficient P2X receptors is subunit dependent -- Hetero-oligomeric $P2X_{2/3}$ channels have unique biophysical and pharmacological properties (sensitivity to the agonist $\alpha\beta$meATP and slow desensitization kinetics) that makes them easily distinguishable from the homo-oligomeric $P2X_2$ and $P2X_3$ receptors. Our results show that co-expression of $P2X_3$ with $P2X_2$[K366A] rescues the lack of function of the mutated $P2X_2$ subunits in a heteromeric channel. A similar rescue is observed with zebrafish $P2X_2$ and $P2X_3$ subunits (3). $zP2X_2$ has no function when expressed as a homo-oligomeric channel, presumably because it lacks the trafficking motif in its C-terminal tail and/or a critical lysine implicated in ATP binding (13); on the other hand, ATP induces typical $P2X_3$-like fast-desensitizing currents at $zP2X_3$. When both $zP2X_2$ and $zP2X_3$ subunits are co-expressed, ATP induces non-desensitizing currents typical of $P2X_{2/3}$ receptors. These results as well as our presents findings provide strong evidence that in the hetero-oligomeric $P2X_{2/3}$ channel the $P2X_2$ subunit is not directly implicated in ATP-induced gating, but rather that binding to the $P2X_3$ subunit alone is responsible for the channel activation. This is further supported by the observation that hetero-oligomeric $P2X_{2/3[K357A]}$ channels could not be activated by $\alpha\beta$meATP. The most probable interpretation for the lack of functional rescue of $P2X_3$[K357A] subunit by Wt $P2X_2$ is that $P2X_2$ and $P2X_3$ subunits do not participate equally in the receptor complex and, that at least two functional subunits are necessary for a channel to gate normally. An alternative explanation is that $P2X_3$[K357A] channel is not able to confer $\alpha\beta$meATP sensitivity to the hetero-oligomeric channel but can still be activated by ATP. This is unlikely since homo-oligomeric $P2X_3$[K357A] channels are not activated by 30 μM or 1 mM ATP (see Fig. 3, and data not shown). However, this question will be difficult to address

experimentally since in co-expression experiments ATP does not discriminate between homo-oligomeric $P2X_2$ and hetero-oligomeric $P2X_{2/3}$ channels.

Mutation of the YXXXK motif destabilized surface expression of $P2X_2$ subunits -- Mutations of the YXXXK motif reduce the surface expression of all homomeric P2X tested. Such a reduction may have different causes such as a misfolding of the protein leading to its degradation, a reduction in the forward trafficking of the protein during its biosynthesis or a lack of stabilization of the receptors at the plasma membrane. The two first possibilities seem unlikely. Thus, we never noticed any decrease in the total cellular content of mutated subunits when compared with wild type subunits as assayed either by western blotting or by luminescence assay (see Fig. 1C); this rules out a misfolding and/or degradation of mutated P2X subunits. By comparison, a $P2X_2$ subunit that lacks glycosylation sites presents a trafficking defect (5), that can be attributed, at least in part, to a misfolding of the protein, because a reduction in the total cellular content of the non glycosylated channel is observed[2]. In addition, it is likely that a misfolded subunit would have not form an oligomeric receptor, nor retained any channel activity. Our results show that mutant $P2X_2$ subunits are able to co-immunoprecipitate and to some extent can be activated by ATP (see Fig. 2). The forward trafficking of mutant P2X receptors is not impaired. Indeed, our pulse-chase experiments clearly demonstrate that mutant P2X receptors acquire complex sugars resistant to endoglycosidase H. This clearly indicates that these proteins are able to travel from the ER to the Golgi apparatus where endoglycosidase H-resistant sugars are added. The rate of forward trafficking of mutant P2X subunits is not likely to be affected since we did not observe any differences in the rate at which mature glycosyl residues are added to WT or trafficking deficient subunits. A reduced forward trafficking rate can therefore not

explain the residual membrane expression of mutant P2X subunits that we consistently observed. We can not exclude that mutant P2X subunits accumulate in the Golgi network; however, such subcellular location would have been noticed in our immuno-staining experiments as a marked difference compared to the Wt P2X subunit cellular distribution.

Our results show that mutant P2X receptors have a reduced surface expression because of a reduced residency time at the cell surface. Indeed, we show that mutant $P2X_2$ subunits are significantly internalized over a period as short as 30 min whereas Wt $P2X_2$ shows very little endocytosis as already described (17). This internalization of $P2X_2$ mutant subunits is not likely mediated by clathrin-mediated endocytosis since these mechanisms are based on the recognition by the endocytic machinery of tyrosine based motifs. This is clearly not the case for mutant P2X subunits in which the deletion of a tyrosine residue promotes internalization. The most likely interpretation for these results is that mutant P2X receptors are internalized though clathrin-independent or fluid-phase endocytosis. We believe that after their endocytosis mutant subunits are recycled to the plasma membrane; this could explain the residual surface expression that we observed for all mutant P2X subunits that were analyzed. Because we did not observe any difference in the total cellular content between mutant and Wt subunits, it is not likely that internalized P2X mutant receptors are directed to the lysosomal pathway. Clathrin-independent internalization and recycling of D2 dopamine receptor has been demonstrated, however the mechanism underlying this type of endocytosis remains unexplained (34).

We propose that the YXXXK motif stabilizes P2X receptors at the plasma membrane. This interpretation is supported by our experiments using CD4 protein

fused either with $P2X_2$ or $P2X_3$ C-terminal. These CD4-fusion proteins display higher surface expression than Wt CD4, that return to normal level when the YXXXK motif is mutated. Because the YXXXK is not involved in the forward trafficking of P2X receptors it is most likely that it enhances CD4 residency time at the plasma membrane by promoting its stabilization (presumably by interactions with cytoskeletal proteins).

There are several examples of stabilization of G protein-coupled receptors (GPCR) or ion channel proteins by interaction with cytoskeletal or scaffolding proteins (for review, 35). For instance, dopamine D_2 receptor or the inward rectifier Kir2.1 channels have been shown to interact with filamin A, an actin-binding protein. This interaction promotes their surface expression by increasing their half-life at the plasma membrane (35). Similarly Kv1.4 potassium channels undergo constitutive internalization unless it is stabilized by co-expression with the scaffolding protein PSD-95 (36,37). Membrane stability of ligand-gated channels might also be promoted by interactions with intracellular proteins that regulate membrane turnover and degradation of the receptor. Indeed, α and β $GABA_A$ subunits are stabilized at the plasma membrane through a direct interaction with Plic-1, an ubiquitin-like protein (38). Although we cannot exclude that P2X subunits interact through the YXXXK motif with a stabilizing protein such as Plic-1, $P2X_2$ subunits do not interact with Plic-1 and protease inhibitors had not effect on the number of wild type or mutant $P2X_2$ subunits at the cell surface (not shown).

The YXXXK motif is involved in the polarized expression of $P2X_2$ in neurons -- Interactions of membrane protein with cytoskeletal or scaffolding proteins not only promote their stabilization but also determine their subcellular expression in polarized cells. We found that the YXXXK motif of the $P2X_2$ receptor regulates their surface

expression and polarization in neurons. Because this motif is present in all P2X receptors, it is unlikely that it represents a true dendritic trafficking motif. Rather, we think that P2X receptors are stabilized at the plasma membrane through interactions with intracellular proteins that might have a polarized expression depending upon the cell type. Such a hypothesis is supported by results obtained on the polarized expression of α_{2B}-adrenergic receptors. These receptors are stabilized at the basolateral membrane of MDCK cells through interaction with the scaffolding protein spinophilin. Mutant α_{2B}-adrenergic receptors that do not interact with spinophilin display an enhanced rate of internalization. However, the artificial targeting of spinophilin to the apical membrane also promotes the redistribution Wt α_{2B}-adrenergic receptors to that surface (39). Interactions of the YXXXK motif with specific cytoskeletal proteins might promote the stabilization and the polarization of P2X receptors to specialized membrane domains.

The YXXXK motif is too degenerate to be used in data mining. We searched databases with a more stringent pattern (LI)-(LV)-X_8-Y-X_3-K in which the double hydrophobic residues helps to anchor the motif near the membrane (see Fig. 1). This pattern is still not very stringent, but we identified the motif in several membrane proteins, usually at the interface between a transmembrane domain and a cytoplasmic region. Interestingly, in the three α_2-adrenergic receptors this pattern is found in the proximal region of their third intracellular loop where basolateral trafficking and stabilization signals have been located. The pattern is also present in intracellular regions of other G protein-coupled receptors such as the serotonin 5-HT_4, the cannabinoid CB_1 or the chemokine CCR7 receptors. The pattern is also found in other membrane proteins such as the sodium channel α subunit SCN8, chloride channels CLC3, 4 and 5, single transmembrane domain proteins such as

NCAM or atrial natriuretic peptide clearance receptor I_B, as well as different kinds of transporters. The presence of the pattern in the third loop of α_2-adrenergic receptors suggest that it might represent a protein-protein interaction domain involved in stabilization of subset of membrane proteins.

In summary, we have identified in P2X receptors a conserved motif that is involved in their surface expression. This motif is necessary for the stabilization of these receptors at the cell surface likely through direct interactions with intracellular proteins. In addition we provide evidence that $P2X_2$ polarized expression in neurons is also related to the presence of this trafficking motif.

Acknowledgments

We thank Dr B. Schwappach for the different CD4 plasmids and for her advice with chemiluminescence assays. This work was supported in part by Fondation pour la Recherche Medicale (F.R.) and The Wellcome Trust (R.A.N.). S.C. was supported by a postgraduate fellowship from Ministère de l'Education Nationale et de la Recherche.

REFERENCES

1. Buell, G., Collo, G., and Rassendren, F. (1996) *Eur J Neurosci* **8**, 2221-2228
2. North, R. A. (2002) *Physiol Rev* **82**, 1013-1067
3. Kucenas, S., Li, Z., Cox, J. A., Egan, T. M., and Voigt, M. M. (2003) *Neuroscience* **121**, 935-945
4. Khakh, B. S. (2001) *Nat Rev Neurosci* **2**, 165-174
5. Newbolt, A., Stoop, R., Virginio, C., Surprenant, A., North, R. A., Buell, G., and Rassendren, F. (1998) *J Biol Chem* **273**, 15177-15182
6. Torres, G. E., Egan, T. M., and Voigt, M. M. (1998) *FEBS Lett* **425**, 19-23
7. Nicke, A., Baumert, H. G., Rettinger, J., Eichele, A., Lambrecht, G., Mutschler, E., and Schmalzing, G. (1998) *Embo J* **17**, 3016-3028
8. Stoop, R., Thomas, S., Rassendren, F., Kawashima, E., Buell, G., Surprenant, A., and North, R. A. (1999) *Mol Pharmacol* **56**, 973-981
9. Jiang, L. H., Kim, M., Spelta, V., Bo, X., Surprenant, A., and North, R. A. (2003) *J Neurosci* **23**, 8903-8910
10. Rassendren, F., Buell, G., Newbolt, A., North, R. A., and Surprenant, A. (1997) *Embo J* **16**, 3446-3454
11. Egan, T. M., Haines, W. R., and Voigt, M. M. (1998) *J Neurosci* **18**, 2350-2359
12. Jiang, L. H., Rassendren, F., Spelta, V., Surprenant, A., and North, R. A. (2001) *J Biol Chem* **276**, 14902-14908
13. Jiang, L. H., Rassendren, F., Surprenant, A., and North, R. A. (2000) *J Biol Chem* **275**, 34190-34196
14. Ennion, S., Hagan, S., and Evans, R. J. (2000) *J Biol Chem* **275**, 29361-29367
15. Werner, P., Seward, E. P., Buell, G. N., and North, R. A. (1996) *Proc Natl Acad Sci U S A* **93**, 15485-15490
16. Koshimizu, T., Koshimizu, M., and Stojilkovic, S. S. (1999) *J Biol Chem* **274**, 37651-37657
17. Bobanovic, L. K., Royle, S. J., and Murrell-Lagnado, R. D. (2002) *J Neurosci* **22**, 4814-4824
18. Royle, S. J., Bobanovic, L. K., and Murrell-Lagnado, R. D. (2002) *J Biol Chem* **277**, 35378-35385
19. Jones, C. A., Vial, C., Sellers, L. A., Humphrey, P. P., Evans, R. J., and Chessell, I. P. (2004) *Mol Pharmacol* **65**, 979-985
20. Bo, X., Jiang, L. H., Wilson, H. L., Kim, M., Burnstock, G., Surprenant, A., and North, R. A. (2003) *Mol Pharmacol* **63**, 1407-1416
21. Ennion, S. J., and Evans, R. J. (2002) *Mol Pharmacol* **61**, 303-311
22. Torres, G. E., Egan, T. M., and Voigt, M. M. (1998) *Biochemistry* **37**, 14845-14851
23. Denlinger, L. C., Sommer, J. A., Parker, K., Gudipaty, L., Fisette, P. L., Watters, J. W., Proctor, R. A., Dubyak, G. R., and Bertics, P. J. (2003) *J Immunol* **171**, 1304-1311
24. Wiley, J. S., Dao-Ung, L. P., Li, C., Shemon, A. N., Gu, B. J., Smart, M. L., Fuller, S. J., Barden, J. A., Petrou, S., and Sluyter, R. (2003) *J Biol Chem* **278**, 17108-17113
25. Zerangue, N., Schwappach, B., Jan, Y. N., and Jan, L. Y. (1999) *Neuron* **22**, 537-548
26. Schwappach, B., Zerangue, N., Jan, Y. N., and Jan, L. Y. (2000) *Neuron* **26**, 155-167

27. Smith, F. M., Humphrey, P. P., and Murrell-Lagnado, R. D. (1999) *J Physiol* **520 Pt 1**, 91-99
28. Lewis, C., Neidhart, S., Holy, C., North, R. A., Buell, G., and Surprenant, A. (1995) *Nature* **377**, 432-435
29. Radford, K. M., Virginio, C., Surprenant, A., North, R. A., and Kawashima, E. (1997) *J Neurosci* **17**, 6529-6533
30. Brandle, U., Spielmanns, P., Osteroth, R., Sim, J., Surprenant, A., Buell, G., Ruppersberg, J. P., Plinkert, P. K., Zenner, H. P., and Glowatzki, E. (1997) *FEBS Lett* **404**, 294-298
31. Toth-Zsamboki, E., Oury, C., Watanabe, H., Nilius, B., Vermylen, J., and Hoylaerts, M. F. (2002) *FEBS Lett* **524**, 15-19
32. Parker, K. E. (1998) *J Physiol* **510 (Pt 1)**, 19-25
33. Ma, D., Zerangue, N., Raab-Graham, K., Fried, S. R., Jan, Y. N., and Jan, L. Y. (2002) *Neuron* **33**, 715-729
34. Vickery, R. G., and von Zastrow, M. (1999) *J Cell Biol* **144**, 31-43
35. Lin, R., Karpa, K., Kabbani, N., Goldman-Rakic, P., and Levenson, R. (2001) *Proc Natl Acad Sci U S A* **98**, 5258-5263
36. Jugloff, D. G., Khanna, R., Schlichter, L. C., and Jones, O. T. (2000) *J Biol Chem* **275**, 1357-1364
37. Sampson, L. J., Leyland, M. L., and Dart, C. (2003) *J Biol Chem* **278**, 41988-41997
38. Bedford, F. K., Kittler, J. T., Muller, E., Thomas, P., Uren, J. M., Merlo, D., Wisden, W., Triller, A., Smart, T. G., and Moss, S. J. (2001) *Nat Neurosci* **4**, 908-916
39. Brady, A. E., Wang, Q., Colbran, R. J., Allen, P. B., Greengard, P., and Limbird, L. E. (2003) *J Biol Chem* **278**, 32405-32412

Footnotes

[1]Abbreviations: C-Term, carboxy terminal; HEK, human embryonic kidney; PBS, phophate buffer saline; FITC, fluorescein isothiocyanate; COS cells, african green monkey kidney cells; GFP, green fluorescent protein; BSA, bovine serum albumin; Cy3, cyanine 3; Wt, wild type; α,βmeATP, alpha,beta metyleneATP; ER, endoplasmicreticulum. [2] F.R., S.C. unpublished observations.

Legends to figures

FIG. 1. **A conserved motif is involved in surface expression of $P2X_2$ subunits**. (A) Partial alignment of the second transmembrane and proximal cytoplamic regions of the seven rat P2X subunits. The membrane-spanning region is indicated by the horizontal bar: conserved residues are indicated by amino acids above the alignment. YXXXK is the only conserved motif found in cytoplasmic C-terminal sequence of P2X subunits. (B) Mutations of the conserved C-terminal motif decrease $P2X_2$ surface expression. Wild type $P2X_2$, $P2X_2$[K366A] and $P2X_2$[Y362A] were expressed in HEK cells; all subunits carried an extracellular Flag epitope (see Methods). Immuno-staining was performed on living cells using a biotinylated anti-Flag antibody and streptavidin Texas-Red prior to cells fixation. Staining of mutant $P2X_2$ subunits was strongly reduced compared to wild type subunits. Note the typical punctated staining that is obtained when the antibody is incubated with living cells. Insets show Flag immunostaining on fixed and permeabilized cells. No difference could be observed between cell expressing wild type or mutant P2X2 subunits (C) Quantification of $P2X_2$ surface expression. Chemiluminescence assay was performed on transfected HEK cells using peroxidase-coupled anti Flag antibody. Black bars represent luminescence signal from permeabilized cells and and gray bars from non-permeabilized cells transfected with Wt and mutant $P2X_2$ subunits. On non-permeablized cells, the [K366A] and [Y362A] mutations induce a strong reduction of the luminescence signal compared to wild type $P2X_2$; this is not seen with permeabilized cells. rlu: relative luminescent units. (D) Alanine-scanning of $P2X_2$ proximal C-terminal tail. All residues from position 360 to 369 were mutated to alanine and their surface expression expressed as the ratio of luminescence signals

from permeabilized and non-permeabilized cells; this gives a direct measure of the proportion of subunits present at the cell surface. Note that only [K366A] and [Y362A] mutants have a reduced surface expression. In all panels bars indicate means ± SEM. *** p<0.001, Student's *t*-test.

FIG. 2. **Y362 and K366 are obligatory residues for surface and functional expression of $P2X_2$ receptors.** Different amino acids substitutions were introduced at the Y362 and K366 positions in the $P2X_2$ subunit. (A) Quantification of the surface expression of $P2X_2$ mutants by chemiluminescence assay. Note that even conservative changes such as Y362F or K366R show reduced surface expression. (B) Mutations of Y362 and K366 residues impair $P2X_2$ channels function. Currents were recorded following applications of 30μM ATP for two seconds (horizontal black bars). Currents could only be recorded from cell transfected with Y362A and Y362F $P2X_2$ mutants. Note the difference in the current scale. The sensitivity to ATP for these mutants was unchanged (not shown). Note the mark desensitization of the currents for $P2X_2$[Y362A]. (C) Current density of $P2X_2$[Y362A] and $P2X_2$[Y362F] were reduced to approximately 30% of Wt $P2X_2$ currents. (D) [K366A] mutation does not affect subunit oligomerization. Co-immunoprecipitation was performed between co-expressed $P2X_2$ Wt and [K366A] subunits. The immunoprecipitation was performed with anti-Flag antibody and immunoblot with anti-Myc antibody. Combinations of subunits that were transfected are indicated above the blot. In all situations, co-immunoprecipitation of subunits was obtained indicating that the K366A mutation does not impair subunit assembly. Bars indicates means ± SEM *** p<0.001, ** p<0.002 Student's *t* test.

FIG. 3. **The YXXXK motif regulates surface expression of other P2X receptors.** Mutations to alanine of the conserved tyrosine and lysine residues were introduced in $P2X_3$, $P2X_4$, $P2X_5$ and $P2X_6$ subunits carrying extracellular epitopes tags. (A) Surface expression of mutant P2X subunits were analyzed by chemiluminescence assays and normalized to the surface expression of their respective Wt subunits. All mutant P2X subunits have a reduced surface expression that range around 35% of Wt subunits (note that for $P2X_6$ 60% of the protein is present at the cell surface but total amounts of the Wt $P2X_6$ subunit were very low compared to the others). Mutant $P2X_3$ and $P2X_4$ subunits are not functional. Currents induced by ATP (30 μM) were recorded from HEK cells transfected with Wt and mutant $P2X_3$ (B) or $P2X_4$ (C) subunits. ATP did not elicit currents in any even at a concentration up to 1 mM. $P2X_5$ and $P2X_6$ Wt subunit did not express functionally. Bars indicates means ± SEM, *** $p<0.001$, ** $p<0.05$ Student's *t* test.

FIG. 4. **Surface expression of trafficking deficient P2X subunits are rescued by co-expression with wild type subunits in heteromeric channels.** Wt and mutant $P2X_2$ and $P2X_3$ subunits were co-expressed in HEK cells; mutant subunits carried an extracellular epitope tag. (A) Surface immuno-staining of $P2X_2$[K366A] is rescued by co-expression with Wt $P2X_3$. Live cell immuno-staining was performed as described in Fig. 1. Almost no $P2X_2$[K366A] staining is observed when the subunit is expressed alone (left panel) whereas strong immunoreactivity appears when $P2X_2$[K366A] and $P2X_3$ are co-expressed (right panel). (B) Differential functional rescue of $P2X_2$[K366A] and $P2X_3$[K357A] mutants in heteromeric $P2X_{2/3}$ channels. Wt or mutant $P2X_2$ and $P2X_3$ subunits were co-expressed in HEK cells. Currents induced by $\alpha\beta$meATP (30 μM; horizontal bars) were recorded two days later. From left to

right, αβmeATP induced stable currents at Wt $P2X_{2/3}$ and $P2X_{2[K366A]/3}$ heteromeric channels. No current could be induced at $P2X_{2/3[K357A]}$ receptors even when concentrations of αβmeATP up to 1 mM were used. αβmeATP currents at homo-oligomeric $P2X_2$ and $P2X_3$ channels are shown; note that $P2X_{2[K366A]/3}$ currents present faster desensitization compared to Wt $P2X_{2/3}$. (C) Surface expression of $P2X_2$[K366A] and $P2X_3$[K357A] subunits are rescued in the hetero-oligomeric channel. Surface expression of mutated $P2X_2$ and $P2X_3$ was quantified as indicated in Fig. 1. When subunits were co-expressed, only the mutated one carried an extracellular Flag ($P2X_2$) or Myc ($P2X_3$) tag. Both $P2X_3$ and $P2X_2$ mutant surface expression is rescued in hetero-oligomeric channels. Results are expressed relative to the surface expression of Wt subunits. Bars indicates means ± SEM, *** $p<0.001$ Student's *t* test.

FIG. 5. **Mutant $P2X_2$ subunits are not retained in the endoplasmic reticulum.** (A) Co-localization of $P2X_2$-GFP C-terminal fusion proteins with the ER marker calreticulin. Co-localization experiments were performed 48 h after transfection of COS cells with either wild type $P2X_2$-GFP, [K366A] and [Y362A] mutants. Wt $P2X_2$-GFP fluorescence is observed at the cell surface as well as in intracellular compartments where it overlaps with calreticulin staining. $P2X_2$-GFP mutant subunits are not present at the plasma membrane. No difference could be observed in the intracellular localization of Wt and mutant $P2X_2$ subunits that clearly co-localized with clareticulin in the Golgi apparatus (perinuclear staining). Cells that have no GFP fluorescence have not been transfected. (B) Mutant $P2X_2$ subunits acquire mature glycosylation. Pulse-chase analysis was performed in transfected HEK cells using S^{35}-labeled methionine. After different time chase protein extracts were treated or

not with endoglycosidaseH. At time zero, glycosylation of all $P2X_2$ subunits can be removed by EndoH as indicated by the mobility shift on the autoradiography. EndoH resistant sugars are added after an hour chase. Note that Wt and mutant subunits show a similar pattern of glycosylation.

FIG. 6. **$P2X_2$ mutant subunits are not stabilized at the cell surface.** (A) Subunit internalization was studied in HEK stable cell lines expressing $P2X_2$ Wt or mutant subunits. All subunits carried an extracellular Flag epitope. Cells were incubated with anti-Flag antibody for 30 min at 37 °C. Surface expressed receptor was detected using a FITC labeled secondary antibody prior cell fixation. Internalized receptors were visualized following fixation with a Cy3 labeled secondary antibody. Images are confocal optical sections of the different fluorophores. Both $P2X_2$[Y362A] and [K366A] subunits show intense intracellular staining compared to Wt $P2X_2$ expressing cells. Line scan fluorescence analysis (right panel) indicates that surface expression of mutant subunits is drastically reduced whereas intracellular signal is increased compare to Wt subunits. A.U. = arbitrary units. (B) The P2X YXXXK motif enhances CD4 surface expression. Fusion between CD4 and the C-terminal tails of P2X subunits were expressed in HEK cells. Surface expression of CD4 and CD4-P2X C-terminal fusions were analyzed by chemiluminescence assay. Top panel, cartoon describing the different CD4 constructions used and their orientation in the plasma membrane. CD4 carries an AAXX sequence at its C-terminal extremity and is normally exported to the cell surface. Wt and mutated C-terminal tail of $P2X_2$, splice variant $P2X_{2b}$ and $P2X_3$ were fused to the carboxyterminus of CD_4. Bottom panel shows surface expression of CD4-C-terminal fusions expressed as % of CD4-AAXX membrane expression. All CD4 fused to Wt C-terminal P2X tails showed an

enhanced surface expression. When the YXXXK motif was mutated surface expression of CD4 fusions were not different from CD4-AAXX (CD_4-$P2X_3$ and CD_4-$P2X_{2b}$) or decreased in the case of CD4-$P2X_2$. In this latter case the use of the splice variant $P2X_{2b}$ indicates that a retention signal in the splice exon is likely to exist. Bars indicates means ± SEM, ** p<0.005 Student's *t* test. Tmd = transmembrane domain.

FIG. 7. **Mutant $P2X_2$ subunits have a reduced surface expression and an altered polarization in transfected neurons**. Embryonic hippocampal neurons ten days culture were transfected with Wt and mutant $P2X_2$-GFP subunits carrying an extracellular Flag epitope. Neurons were fixed 48 h after transfection. (A) reduced surface expression of $P2X_2$ mutant subunits in neurons. Left panel, total and cell surface distribution of $P2X_2$ subunits were visualized through GFP fluorescence and Flag immuno-staining on non-permeabilized cells, respectively. Both Wt and mutant $P2X_2$ subunits localized in varicosities even in distal regions of processes. Wt but not mutant subunits are expressed at the cell surface of varicosities. Arrows indicate processes that are GFP and Flag positives. Right panel, the number of double fluorescent varicosities were quantified using the Image J software as indicated in the methods section. Bars indicates means ± SEM, ** p<0.005 Student's *t* test. (B) Altered polarization of mutant $P2X_2$ subunits in neurons. Co-localization of Wt and mutant $P2X_2$ subunits and the dendritic marker MAP2 was analyzed in transfected neurons. Wt $P2X_2$ subunits $P2X_2$ is expressed only in MAP2 positive processes; however, both mutated $P2X_2$ subunits were present in MAP2 negatives processes as indicated by arrows. Images are representative of results obtained from at least three independent cultures.

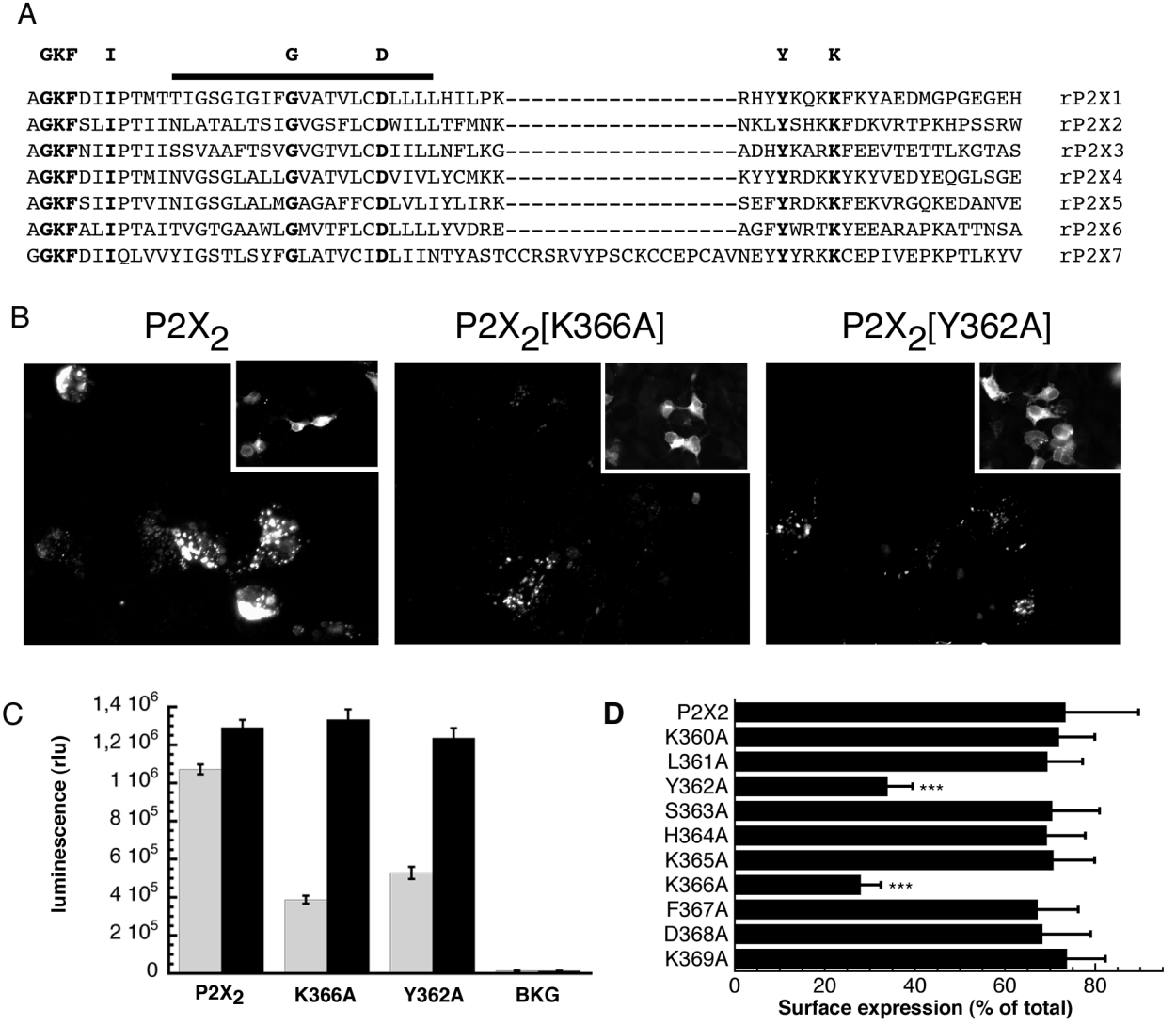
A
GKF I G D Y K
AGKFDIIPTMTTIGSGIGIFGVATVLCDLLLLHILPK----------RHYYKQKKFKYAEDMGPGEGEH rP2X1
AGKFSLIPTIINLATALTSIGVGSFLCDWILLTFMNK----------NKLYSHKKFDKVRTPKHPSSRW rP2X2
AGKFNIIPTIISSVAAFTSVGVGTVLCDIILLNFLKG----------ADHYKARKFEEVTETTLKGTAS rP2X3
AGKFDIIPTMINVGSGLALLGVATVLCDVIVLYCMKK----------KYYYRDKKYKYVEDYEQGLSGE rP2X4
AGKFSIIPTVINIGSGLALMGAGAFFCDLVLIYLIRK----------SEFYRDKKFEKVRGQKEDANVE rP2X5
AGKFALIPTAITVGTGAAWLGMVTFLCDLLLLYVDRE----------AGFYWRTKYEEARAPKATTNSA rP2X6
GGKFDIIQLVVYIGSTLSYFGLATVCIDLIINTYASTCCRSRVYPSCKCCEPCAVNEYYYRKKCEPIVEPKPTLKYV rP2X7
B
P2X2
P2X2[K366A]
P2X2[Y362A]
C
luminescence (rlu)
1,4 10^6
1,2 10^6
1 10^6
8 10^5
6 10^5
4 10^5
2 10^5
0
P2X2
K366A
Y362A
BKG
D
P2X2
K360A
L361A
Y362A
S363A
H364A
K365A
K366A
F367A
D368A
K369A
***
***
0
20
40
60
80
Surface expression (% of total)

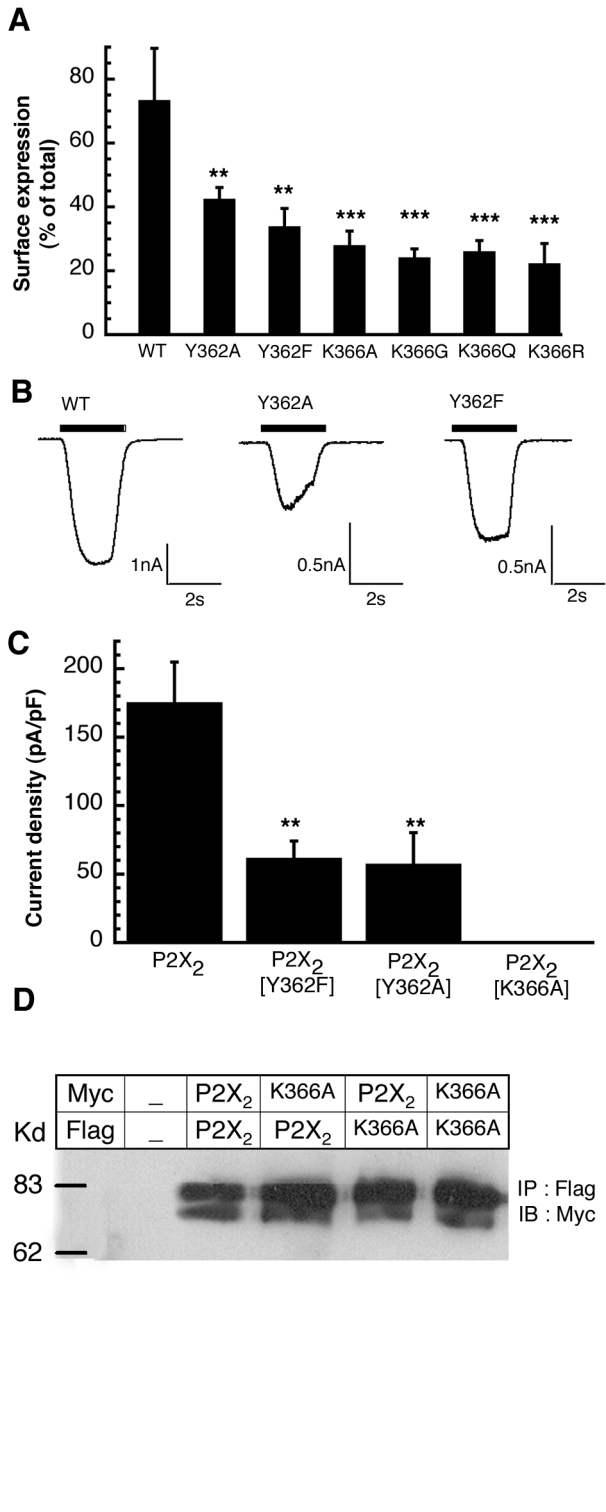
A
Surface expression (% of total)
80
60
40
20
0
**
**
***
***
***
***
WT
Y362A
Y362F
K366A
K366G
K366Q
K366R
B
WT
Y362A
Y362F
1nA
2s
0.5nA
2s
0.5nA
2s
C
Current density (pA/pF)
200
150
100
50
0
**
**
P2X2
P2X2 [Y362F]
P2X2 [Y362A]
P2X2 [K366A]
D
Myc
Flag
Kd
_
_
P2X2
P2X2
K366A
K366A
P2X2
P2X2
K366A
K366A
83
62
IP : Flag
IB : Myc

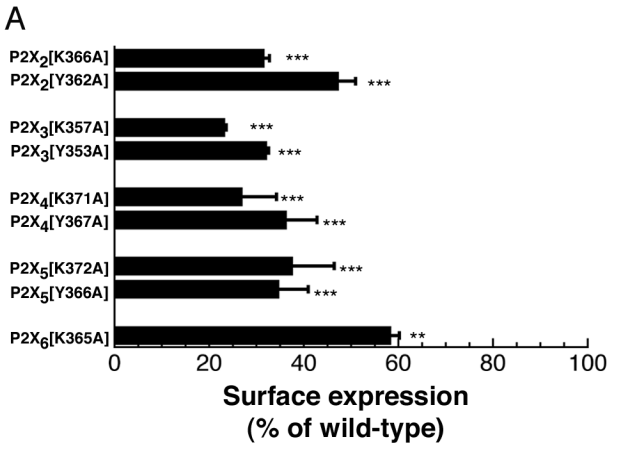
A
P2X2[K366A]
P2X2[Y362A]
P2X3[K357A]
P2X3[Y353A]
P2X4[K371A]
P2X4[Y367A]
P2X5[K372A]
P2X5[Y366A]
P2X6[K365A]
***
***
***
***
***
***
***
***
**
0
20
40
60
80
100
Surface expression
(% of wild-type)

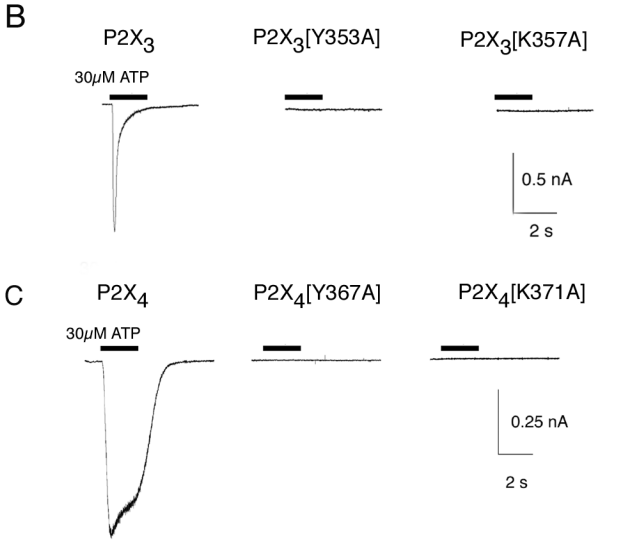
B
P2X3
P2X3[Y353A]
P2X3[K357A]
30μM ATP
0.5 nA
2 s
C
P2X4
P2X4[Y367A]
P2X4[K371A]
30μM ATP
0.25 nA
2 s

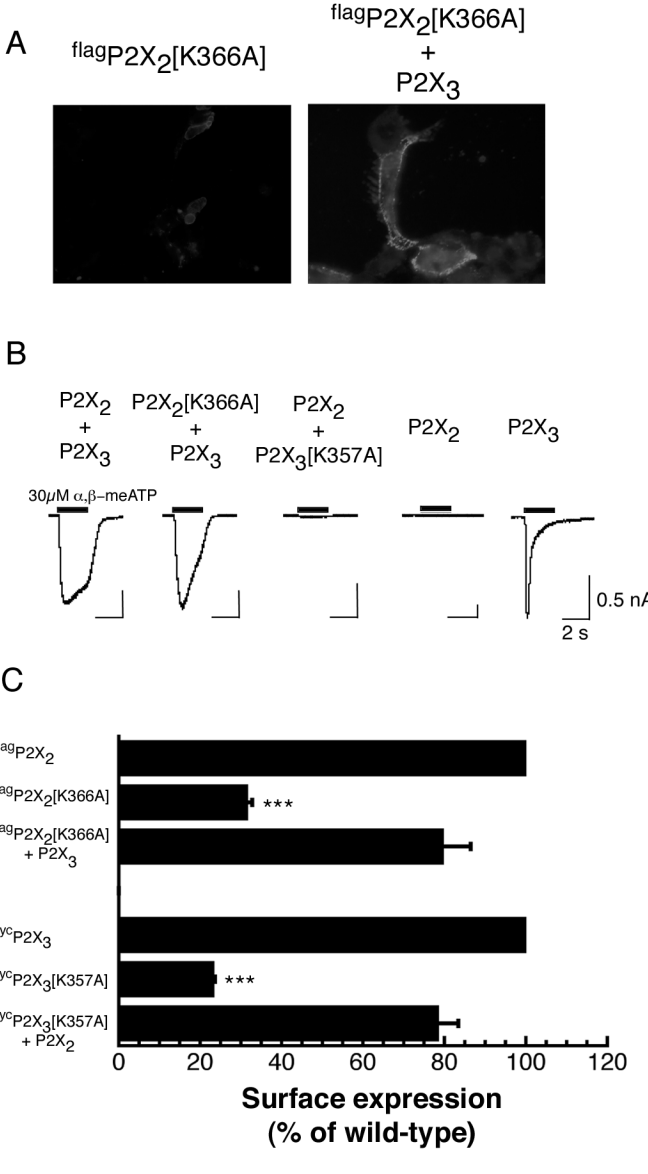
A
flagP2X2[K366A]
flagP2X2[K366A]
+
P2X3
B
P2X2
+
P2X3
P2X2[K366A]
+
P2X3
P2X2
+
P2X3[K357A]
P2X2
P2X3
30μM α,β-meATP
0.5 nA
2 s
C
flagP2X2
flagP2X2[K366A]
***
flagP2X2[K366A]
+ P2X3
mycP2X3
mycP2X3[K357A]
***
mycP2X3[K357A]
+ P2X2
0
20
40
60
80
100
120
Surface expression
(% of wild-type)

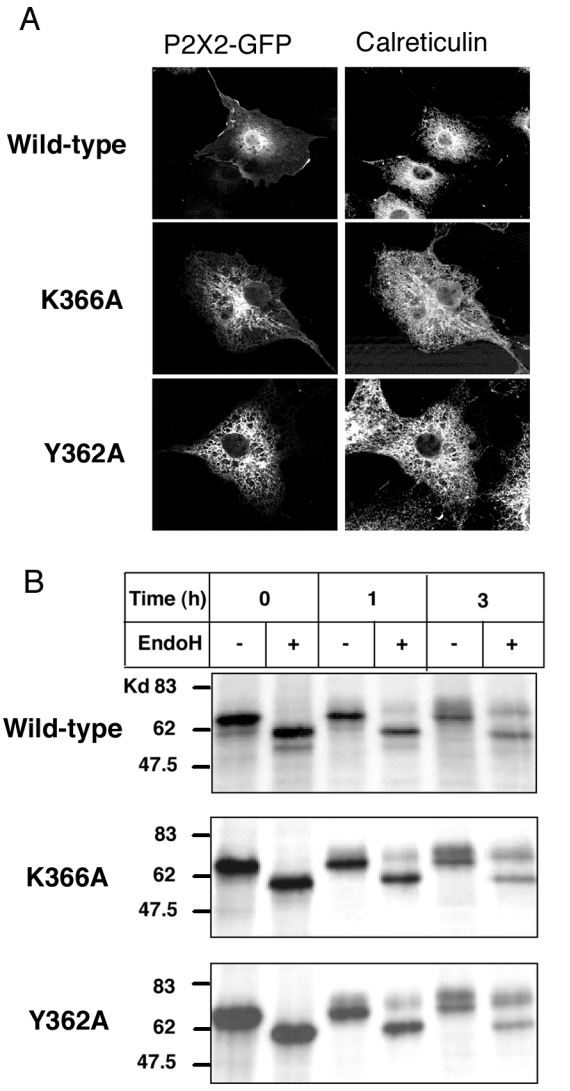
A
P2X2-GFP
Calreticulin
Wild-type
K366A
Y362A
B
Time (h)
0
1
3
EndoH
-
+
-
+
-
+
Kd 83
62
47.5
Wild-type
83
62
47.5
K366A
83
62
47.5
Y362A

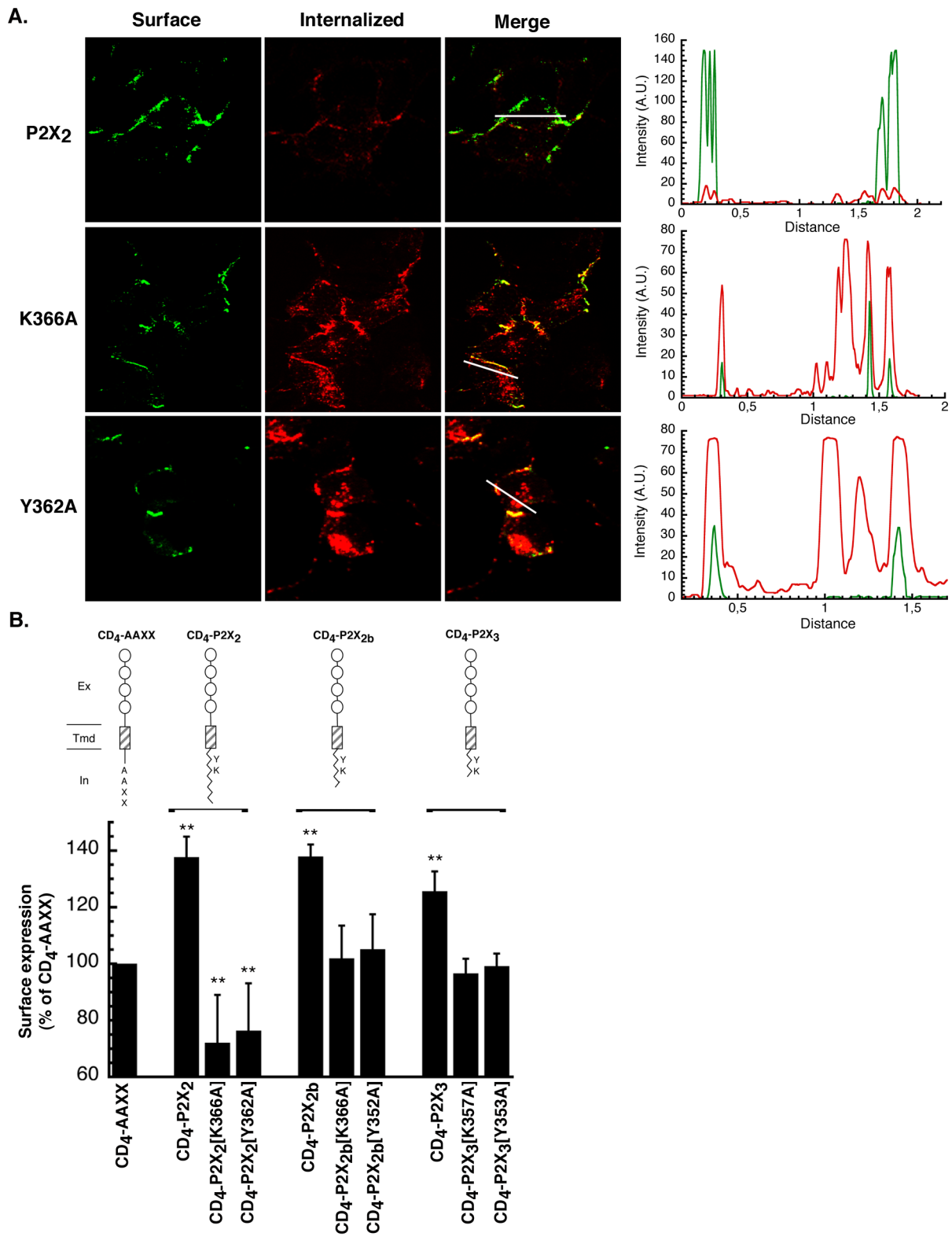
A.
Surface
Internalized
Merge
P2X2
K366A
Y362A
Intensity (A.U.)
Distance
B.
CD4-AAXX
CD4-P2X2
CD4-P2X2b
CD4-P2X3
Ex
Tmd
In
A A X X
Y K
Surface expression (% of CD4-AAXX)
**
CD4-AAXX
CD4-P2X2
CD4-P2X2[K366A]
CD4-P2X2[Y362A]
CD4-P2X2b
CD4-P2X2b[K366A]
CD4-P2X2b[Y352A]
CD4-P2X3
CD4-P2X3[K357A]
CD4-P2X3[Y353A]

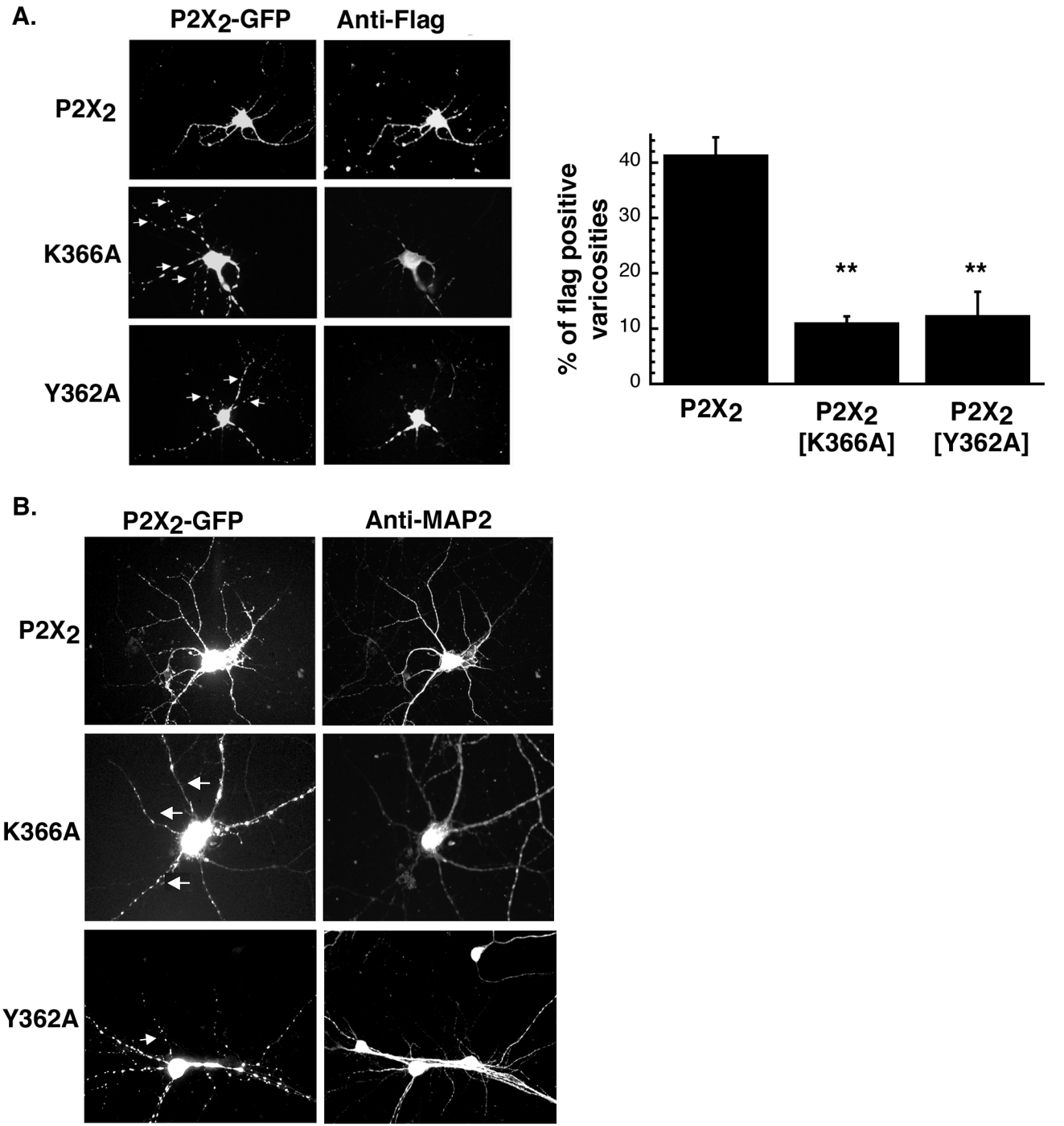
A.
P2X2-GFP
Anti-Flag
P2X2
K366A
Y362A
% of flag positive varicosities
40
30
20
10
0
**
**
P2X2
P2X2 [K366A]
P2X2 [Y362A]
B.
P2X2-GFP
Anti-MAP2
P2X2
K366A
Y362A